NATIONAL ADVISORY COMMITTEE FOR AERONAUTICS

TECHNICAL NOTE 2048

THEORETICAL LIFT AND DAMPING IN ROLL OF THIN SWEPTBACK TAPERED WINGS WITH RAKED-IN AND CROSS-STREAM WING TIPS AT SUPERSONIC SPEEDS

SUBSONIC LEADING EDGES

By Kenneth Margolis

Langley Aeronautical Laboratory
Langley Air Force Base, Va.

Washington
March 1950

NATIONAL ADVISORY COMMITTEE FOR AERONAUTICS

TECHNICAL NOTE 2048

THEORETICAL LIFT AND DAMPING IN ROLL OF THIN SWEPTBACK TAPERED WINGS WITH RAKED-IN AND CROSS-STREAM WING TIPS AT SUPERSONIC SPEEDS SUBSONIC LEADING EDGES

By Kenneth Margolis

SUMMARY

On the basis of linearized supersonic-flow theory, the lift and damping in roll have been evaluated for families of thin sweptback tapered wings with raked-in and cross-stream wing tips. Equations were derived for wings that are wholly contained within a boundary formed by the Mach lines, that is, wings with subsonic leading edges, supersonic trailing edges, and supersonic wing tips. Consideration was given to some classes of wings with subsonic trailing edges and subsonic wing tips.

Design charts are presented which permit rapid estimation of the lift-curve slope C_{L_α} and the damping-in-roll derivative C_{l_p}. Some illustrative variations of the derivatives with aspect ratio, taper ratio, Mach number, and leading-edge sweep are also presented and compared with corresponding data for wings with streamwise tips.

INTRODUCTION

A number of papers dealing with the stability derivatives of various isolated wing configurations have been published to date (for example, references 1 to 8). The present paper considers the lift-curve slope C_{L_α} and the damping-in-roll derivative C_{l_p} for certain plan forms not yet treated in detail.

Equations and formulas, which are subject to the usual restrictions and limitations of linearized thin-airfoil theory, are derived for the

lift and damping in roll of sweptback tapered wings with raked-in and cross-stream wing tips at supersonic speeds. The results are applicable to wings with subsonic leading edges, supersonic trailing edges, and supersonic wing tips.

Calculations are presented in the form of design charts for families of wings with (a) raked-in wing tips, such that the inclinations of the tip and trailing edge from the free-stream direction are equal, and (b) cross-stream wing tips. Approximations for certain types of subsonic trailing edges and subsonic wing tips are included in order to extend the range of design parameters under consideration. Some illustrative variations of the derivatives with the parameters – Mach number, aspect ratio, taper ratio, and leading-edge sweep – are also presented and compared with results for streamwise-tip wings.

SYMBOLS

x,y,z	Cartesian coordinates
V	flight speed
α	angle of attack
p,q,r	angular velocities about X-, Y-, and Z-axes, respectively
M	free-stream Mach number (V/Speed of sound)
$B = \sqrt{M^2 - 1}$	
μ	Mach angle $\left(\text{arc tan } \frac{1}{B}\right)$
ϵ	angle between leading edge and axis of wing symmetry (See fig. 1.)
δ	angle between trailing edge and axis of wing symmetry (See fig. 1.)
σ	rake angle of wing tip (See fig. 1.)
$m_1 = \frac{\tan \epsilon}{\tan \mu} = B \cot \Lambda$	

$$m_2 = \frac{\tan \delta}{\tan \mu} = \frac{m_1}{1 - (1 - \lambda_s)\omega}$$

$$m_3 = \frac{\tan \sigma}{\tan \mu}$$

Λ sweepback angle of leading edge ($90^\circ - \epsilon$)

$\theta_o = \cot \Lambda = \tan \epsilon$

$$\eta = \frac{y}{\theta_o x}$$

b wing span

c_r wing root chord

ω geometric parameter of wing

$$\left(\frac{2c_r\theta_o}{b} = \frac{8m_1}{AB(1 + \lambda_s)\left(1 + \sqrt{1 - \frac{16\lambda_s^2 m_2 m_3}{AB(1 + \lambda_s)^2(m_2 + m_3)}}\right)} \right)$$

S wing area

A aspect ratio (b^2/S)

λ_s taper-ratio parameter (ratio of tip chord to root chord based on fictional wing with streamwise tip; see fig. 1)

ΔP local pressure difference between lower and upper surfaces of airfoil, positive in sense of lift

ρ density

C_P pressure coefficient $\left(\frac{\Delta P}{\frac{1}{2}\rho V^2} \right)$

$k = \sqrt{1 - m_1^2}$

$E'(m_1)$ complete elliptic integral of second kind with modulus k; $\left(\int_0^{\pi/2} \sqrt{1 - k^2 \sin^2 z}\, dz \right)$

$E''(m_1) = \frac{1}{E'(m_1)}$

$F'(m_1)$ complete elliptic integral of first kind with modulus k; $\left(\int_0^{\pi/2} \frac{dz}{\sqrt{1 - k^2 \sin^2 z}} \right)$

$$I(m_1) = \frac{2\left(1 - m_1^2\right)}{\left(2 - m_1^2\right)E'(m_1) - m_1^2 F'(m_1)}$$

L lift

L' rolling moment

C_L lift coefficient $\left(\frac{L}{\frac{1}{2} \rho V^2 S} \right)$

C_l rolling-moment coefficient $\left(\frac{L'}{\frac{1}{2} \rho V^2 S b} \right)$

$$C_{L_\alpha} = \left(\frac{\partial C_L}{\partial \alpha} \right)_{\alpha \to 0}$$

$$C_{l_p} = \left(\frac{\partial C_l}{\partial \frac{pb}{2V}} \right)_{\frac{pb}{2V} \to 0}$$

All angles are measured in radians. Subscripts α and p when used outside of parentheses refer to lift and roll, respectively.

ANALYSIS

Scope

The general type of sweptback plan form treated in the present paper is sketched in figure 1. For convenience, the trailing-edge angle δ and the rake angle σ are restricted to acute angles. The orientation of the wing with respect to a body system of coordinate axes used in the analysis is indicated in figure 2(a). Figure 2(b) shows the wing oriented with respect to the stability axes system. To the first order in α (the angle of attack), the derivatives C_{l_α} and C_{l_p} have the same values in the stability system as they do in the principal body axes system (shown dashed in fig. 2(b)).

The analysis is based on linearized theory and is limited to wings of vanishingly small thickness that have zero camber and are not yawed with respect to the stream direction. The derivatives are exact (within the bounds of linearized theory) for the range of supersonic speeds for which the wing leading edge is subsonic and the wing trailing edge and wing tip are supersonic. (An edge is termed "subsonic" if the stream component normal to the edge is subsonic and is termed "supersonic" if the normal component is supersonic.)

These conditions impose limitations on the angles ϵ, δ, and μ (that is, $\epsilon < \mu$, $\delta > \mu$, and $\sigma > \mu$) that may be expressed as follows:

$$\left.\begin{aligned} & m_3 > 1 \\ & \frac{BA'(1+\lambda_s)}{BA'(1+\lambda_s)+4(1-\lambda_s)} < m_1 < 1 \end{aligned}\right\} \qquad (1)$$

where

$$A' = \frac{A + A\sqrt{1 - \dfrac{16\lambda_s{}^2 m_2 m_3}{(1+\lambda_s)^2(m_2+m_3)AB}}}{2}$$

Consideration is given to some plan forms with subsonic wing tips and subsonic trailing edges. Approximations for the condition of subsonic wing tips are obtained by use of reference 7 and approximations for wings with subsonic trailing edges are based on modifications of both reference 9 and some unpublished work by H. S. Ribner of the Lewis Flight Propulsion Laboratory. The numerical results presented incorporate these corrections wherever practicable, although the mathematical equations developed in the present paper apply specifically to plan forms satisfying the restrictions imposed in equation (1).

Basic Considerations

The evaluation of the derivatives C_{L_α} and C_{l_p} involves essentially a knowledge of the lifting-pressure distribution over the wing associated with angle of attack for C_{L_α} and with rolling for C_{l_p}.

Consider the triangular wing sketched in figure 3(a). If the trailing edge is cut off from the tip to the center line along an angle always greater than the Mach angle, the pressure distribution over the remaining portion of the wing will be unchanged. This fact arises from the nature of the supersonic flow in which disturbances are confined within the Mach cone from the origin of the disturbance. The aforementioned cutting procedure produces therefore a series of sweptback tapered wings having pointed tips (see fig. 3(b)). The plan forms under consideration may now be obtained by cutting off the pointed tips along lines having angles greater than the Mach angle (fig. 3(c)). The pressures over the remaining portion of the wing are exactly the same as if the cutbacks had not been made; that is, the pressure at point (x_o,y_o), for example, remains unchanged.

The appropriate pressure coefficient for the evaluation of the lift-curve slope C_{L_α} may be obtained from consideration of references 10 and 11 and is expressible as:

$$\left(C_p\right)_\alpha = \frac{\Delta P}{\frac{1}{2}\rho V^2} = \frac{4\theta_o\alpha}{E'(m_1)\sqrt{1-\eta^2}} \qquad (2)$$

The pressure coefficient for rolling is derived in reference 12 and is as follows:

$$(C_p)_p = \frac{2p\theta_o{}^2 I(m_1)}{V} \frac{x\eta}{\sqrt{1-\eta^2}} \tag{3}$$

The stability derivatives C_{L_α} and C_{l_p} are then obtained by performing the indicated operations:

$$C_{L_\alpha} = \frac{1}{S} \frac{\partial}{\partial \alpha} \int (C_p)_\alpha \, dS \tag{4a}$$

$$C_{l_p} = \frac{1}{Sb} \frac{\partial}{\partial \frac{pb}{2V}} \int (C_p)_p y \, dS \tag{4b}$$

where the integration is performed over the complete wing.

Lift-Curve Slope C_{L_α}

The particular form of the lifting-pressure coefficient (constant pressure along lines η = Constant - see equation (2)) suggests the polar-integration procedure for the derivation of C_{L_α}. Thus, the wing is considered as composed of an infinite number of elemental triangular areas (see fig. 4). The lift is then determined for each triangular area and the results summed by integration as indicated in equation (4a).

The following geometric relationships will prove useful in setting up the integral and may be readily derived from information given in figure 4. For wing region TOD,

$$\left.\begin{aligned} x_1 &= \frac{c_r m_2}{m_2 - \eta m_1} \\ dy_1 &= \frac{c_r m_2 \theta_o}{m_2 - \eta m_1} d\eta \\ dS &= \frac{1}{2} \theta_o c_r{}^2 m_2{}^2 \frac{d\eta}{(m_2 - \eta m_1)^2} \end{aligned}\right\} \tag{5a}$$

For wing region TOG,

$$\left.\begin{aligned} x_1 &= \frac{b}{2\theta_o}\left(\frac{m_1 + m_3}{m_1\eta + m_3}\right) \\ dy_1 &= x_1\theta_o\, d\eta = \frac{b}{2}\left(\frac{m_1 + m_3}{m_1\eta + m_3}\right)d\eta \\ dS &= \frac{1}{2}\, x_1\, dy_1 = \frac{b^2}{8\theta_o}\left(\frac{m_1 + m_3}{m_1\eta + m_3}\right)^2 d\eta \end{aligned}\right\} \qquad (5b)$$

Equation (4a) may now be rewritten as (see fig. 4 for information pertinent to integration limits)

$$C_{I_\alpha} = \frac{4\theta_o{}^2 c_r{}^2 m_2{}^2}{SE'(m_1)} \int_0^{\frac{m_2}{m_1}\left(\frac{m_1 + m_3 - m_3\omega}{\omega m_2 + m_1 + m_3}\right)} \frac{d\eta}{(m_2 - \eta m_1)^2\sqrt{1 - \eta^2}} +$$

$$\frac{b^2(m_1 + m_3)^2}{SE'(m_1)} \int_{\frac{m_2}{m_1}\left(\frac{m_1 + m_3 - m_3\omega}{\omega m_2 + m_1 + m_3}\right)}^{1} \frac{d\eta}{(m_1\eta + m_3)^2\sqrt{1 - \eta^2}} \qquad (6)$$

Integration and simplification yields

$$BC_{L_\alpha} = \frac{AB}{E'(m_1)} \left\{ \frac{\omega m_2(m_1 - m_3) + (m_1^2 - m_2^2)}{(m_2 + m_3)(m_1^2 - m_2^2)(m_1 - m_3)} \sqrt{m_1^2(m_2\omega + m_1 + m_3)^2 - m_2^2(m_1 + m_3 - m_3\omega)^2} - \right.$$

$$\frac{\omega^2 m_2^3}{(m_2^2 - m_1^2)^{3/2}} \left[\sin^{-1} \frac{m_2\omega(m_1^2 + m_2m_3) + (m_1 + m_3)(m_1^2 - m_2^2)}{m_1m_2\omega(m_2 + m_3)} - \sin^{-1} \frac{m_1}{m_2} \right] +$$

$$\left. \frac{\omega^2 m_1 m_2}{(m_2^2 - m_1^2)} + \frac{m_3\sqrt{m_1 + m_3}}{(m_3 - m_1)^{3/2}} \cos^{-1} \frac{\omega m_2(m_1 - m_3) + (m_1^2 + m_2m_3)}{m_1(m_2 + m_3)} \right\} \qquad (7)$$

For the special case of cross-stream tips – that is, for $m_3 \to \infty$ – equation (7) reduces to

$$BC_{L_\alpha} = \frac{AB}{E'(m_1)} \left\{ \frac{\omega m_2}{m_2^2 - m_1^2} \left[\omega m_1 - \sqrt{m_1^2 - m_2^2(1 - \omega)^2} \right] + \right.$$

$$\left. \frac{\omega^2 m_2^3}{(m_2^2 - m_1^2)^{3/2}} \left(\sin^{-1} \frac{m_1}{m_2} - \sin^{-1} \frac{m_2^2\omega + m_1^2 - m_2^2}{m_1m_2\omega} \right) + \cos^{-1} \frac{m_2(1 - \omega)}{m_1} \right\} \qquad (8)$$

Damping-in-Roll Derivative C_{l_p}

In a manner analogous to the procedure employed in the previous section for C_{L_α}, the rolling moment is determined for an elemental triangle and the result is integrated over the wing area to enable the evaluation of C_{l_p} for the complete wing.

The rolling moment of an elemental triangle is

$$dL' = -y_R \, dL \tag{9}$$

where y_R is the perpendicular distance from the roll axis to the point on the triangle where the resultant lift acts. It can be shown that, when the pressure is of the form $x\,f(\eta)$ (as is indeed the case for rolling – see equation (3)), the resultant lift acts at the $\frac{3}{4}$-chord point of the triangle, that is, at $\frac{3}{4}x_1$.

Since the y-coordinate of this point is

$$y_R = \frac{3}{4} x_1 \theta_o \eta \tag{10}$$

and the lift (due to rolling) on an elemental triangle is

$$dL = \int_0^{x_1} (\Delta P)_p \theta_o \, d\eta \; x \, dx$$

$$= \frac{V p \rho \theta_o {}^3 I(m_1) x_1{}^3}{3} \frac{\eta}{\sqrt{1 - \eta^2}} \, d\eta \tag{11}$$

the following integral form for C_{l_p} may be obtained from consideration of equations (4b), (5), (9), (10), and (11):

$$C_{l_p} = \frac{2}{\rho V^2 S b} \frac{\partial}{\partial \frac{pb}{2V}} \int dL'$$

$$= \frac{-2c_r{}^4\theta_o{}^4 I(m_1) m_2{}^4}{b^2 S} \int_0^{\frac{m_2}{m_1}\left(\frac{m_1 + m_3 - m_3\omega}{\omega m_2 + m_1 + m_3}\right)} \frac{\eta^2 d\eta}{(m_2 - \eta m_1)^4 \sqrt{1 - \eta^2}} -$$

$$\frac{b^2 (m_1 + m_3)^4 I(m_1)}{8S} \int_{\frac{m_2}{m_1}\left(\frac{m_1 + m_3 - m_3\omega}{\omega m_2 + m_1 + m_3}\right)}^1 \frac{\eta^2 d\eta}{(m_3 + \eta m_1)^4 \sqrt{1 - \eta^2}} \quad (12)$$

Integration and simplification yields

$$BC_{l_p} = -\frac{ABI(m_1)}{16}\left[\frac{\omega^4}{(m_1^2-m_2^2)^3}\left(\frac{\left\{\begin{array}{l}m_2^3\left\{(m_1+m_3-\omega m_3)\left[\left(6m_1^4+10m_1^2m_2^2-m_2^4\right)(m_1+m_3-m_3\omega)+(m_2\omega+\right.\right.\right.\\ \left.\left.\left.m_1+m_3)\left(3m_2^4-27m_1^2m_2^2-6m_1^4\right)\right]+m_1^2\left(2m_1^2+13m_2^2\right)(m_2\omega+m_1+m_3)^2\right\}\end{array}\right.}{3m_1^2\omega^3(m_2+m_3)^3}\sqrt{m_1^2(m_2\omega+m_1+m_3)^2-m_2^2(m_1+m_3-m_3\omega)^2}+\right.$$

$$\left.\frac{m_2^5\left(4m_1^2+m_2^2\right)}{\sqrt{m_2^2-m_1^2}}\left[\sin^{-1}\frac{m_2\omega(m_1^2+m_2m_3)+(m_1+m_3)(m_1^2-m_2^2)}{m_1m_2\omega(m_2+m_3)}-\sin^{-1}\frac{m_1}{m_2}\right]-\frac{m_1m_2^3\left(2m_1^2+13m_2^2\right)}{3}\right)+$$

$$\frac{m_3^2(m_1+m_3)}{(m_1-m_3)^3}\left\{\frac{4m_1^2+m_3^2}{m_3\sqrt{m_3^2-m_1^2}}\cos^{-1}\frac{\omega m_2(m_1-m_3)+(m_1^2+m_2m_3)}{m_1(m_2+m_3)}+\frac{\left\{\begin{array}{l}m_2(m_1+m_3-\omega m_3)\left[m_2(m_1+m_3-\omega m_3)\left(6m_1^4+\right.\right.\right.\\ \left.\left.\left.10m_1^2m_3^2-m_3^4\right)+m_3(m_2\omega+m_1+m_3)\left(6m_1^4+\right.\right.\\ \left.\left.27m_1^2m_3^2-3m_3^4\right)\right]+m_1^2m_3^2\left(2m_1^2+13m_3^2\right)(m_2\omega+m_1+m_3)^2\end{array}\right\}}{3m_1^2m_3^2(m_1+m_3)^3(m_2+m_3)^3}\sqrt{m_1^2(m_2\omega+m_1+m_3)^2-m_2^2(m_1+m_3-\omega m_3)^2}\right\}\right] \quad (13)$$

For the special case of cross-stream tips – that is, $m_3 \to \infty$ – equation (13) reduces to

$$BC_{l_p} = -\frac{ABI(m_1)}{16}\left[\frac{\omega^4}{(m_1^2 - m_2^2)^3}\left(-\frac{m_1 m_2^3(2m_1^2 + 13m_2^2)}{3} + \right.\right.$$

$$\frac{\left\{m_2^3\left\{(1-\omega)\left[2m_2^4 - 17m_1^2m_2^2 - \omega(6m_1^4 + 10m_1^2m_2^2 - m_2^4)\right] + m_1^2(2m_1^2 + 13m_2^2)\right\}\sqrt{m_1^2 - m_2^2(1-\omega)^2}\right\}}{3m_1^2\omega^3} +$$

$$\left.\left.\frac{m_2^5(4m_1^2 + m_2^2)}{\sqrt{m_2^2 - m_1^2}}\left[\sin^{-1}\frac{m_1^2 - m_2^2(1-\omega)}{m_1 m_2 \omega} - \sin^{-1}\frac{m_1}{m_2}\right]\right) + \right.$$

$$\left.\cos^{-1}\frac{m_2(1-\omega)}{m_1} + \frac{m_2(1-\omega)}{m_1^2}\sqrt{m_1^2 - m_2^2(1-\omega)^2}\right] \qquad (14)$$

It should be noted that the $I(m_1)$ function present in the formulas for rolling, as well as the $E'(m_1)$ function in the case of lift, are elliptic functions. For purposes of convenience in applying the final formulas, variations of $E''(m_1) = \frac{1}{E'(m_1)}$ and $I(m_1)$ with m_1 are presented in figure 5.

RESULTS AND DISCUSSION

As stated previously, the equations are derived specifically for wings with subsonic leading edges, supersonic trailing edges, and supersonic wing tips. The design charts presented, however, include cases for subsonic wing tips and subsonic trailing edges. The approximations used to correct for the subsonic tips are based on formulas (for wings with streamwise tips) presented in reference 7, modified to take into account differences in wing-tip configurations. The approximations used to correct for certain classes of subsonic trailing edges (those cases where the Mach lines from the apex of the trailing edge intersect the tip) are based on modifications of both reference 9 and some unpublished research. All numerical calculations for the design charts (figs. 6 to 9) based entirely on the equations derived in the present paper are represented by those solid-line portions of the curves to the right of the boundary line. Those computations incorporating the aforementioned corrections and approximations for subsonic tips and subsonic trailing edges are indicated by the solid-line portions of the curves to the left of the boundary line. The dashed portions of the curves (which refer to plan forms with subsonic trailing edges where the Mach lines from the apex of the trailing edge intersect the leading edge) are given merely as a guide and do not represent actual calculations. The sections of the dashed curves adjacent to the solid sections are believed to give fair approximations; the sections of the dashed curves remote from the solid sections may be quite inaccurate and should be used only as rough approximations. Information relative to the quantitative evaluation of the lift and damping in roll for such cases may be found in references 13 and 14, respectively.

Two types of raked-in tips were considered for calculation purposes: the special case of cross-stream tips $\left(\sigma = \frac{\pi}{2}\right)$ for which the geometric parameter ω becomes

$$\omega_{\sigma=\frac{\pi}{2}} = \frac{4m_1\left(1 - \lambda_s\right) + AB\left(1 + \lambda_s\right) - \sqrt{A^2B^2\left(1 + \lambda_s\right)^2 - 8m_1AB\left(1 + \lambda_s^2\right) + 16m_1^2\left(1 - \lambda_s\right)^2}}{2AB} \tag{15a}$$

and the case where the rake angle equals the trailing-edge angle ($\sigma = \delta$) for which the parameter ω is expressible as

$$\omega_{\sigma=\delta} = \frac{4m_1\left(1 - \lambda_s\right) + AB\left(1 + \lambda_s\right) - \sqrt{A^2B^2\left(1 + \lambda_s\right)^2 - 8ABm_1 + 16m_1^2\left(1 - \lambda_s\right)^2}}{AB\left(2 - \lambda_s^2\right)} \tag{15b}$$

Inasmuch as $m_1 = B \cot \Lambda$ and $m_2 = \frac{m_1}{1 - \left(1 - \lambda_s\right)\omega}$, the derived formulas for BC_{l_α} (equations (7) and (8)) and BC_{l_p} (equations (13) and (14)) are readily seen to be functions of the parameters AB, B cot Λ, and λ_s. Design charts were prepared in terms of these parameters and are presented in figures 6 to 9. Figures 6 and 7 present lift-curve-slope calculations of the wings with raked-in tips ($\sigma = \delta$) and cross-stream tips $\left(\sigma = \frac{\pi}{2}\right)$, respectively; corresponding charts for damping in roll are given in figures 8 and 9.

For illustrative purposes, some specific variations of the derivatives C_{L_α} and C_{l_p} with each of the parameters – aspect ratio, taper ratio, Mach number, and leading-edge sweep – are presented in figures 10 and 11, respectively. Comparison with results obtained from reference 7 for streamwise tips is indicated in each figure.

CONCLUDING REMARKS

On the basis of the linearized theory for supersonic flow, the lift-curve slope C_{L_α} and the damping-in-roll derivative C_{l_p} have been evaluated for families of thin sweptback tapered wings with raked-in and cross-stream wing tips for a limited range of supersonic speeds.

Results of the analysis are presented in the form of design charts which permit rapid estimation of the derivatives. Some illustrative variations of the derivatives with aspect ratio, taper ratio, Mach number, and leading-edge sweep are also presented and compared with corresponding data for wings with streamwise tips.

Langley Aeronautical Laboratory
National Advisory Committee for Aeronautics
Langley Air Force Base, Va., December 8, 1949

REFERENCES

1. Ribner, Herbert S.: The Stability Derivatives of Low-Aspect-Ratio Triangular Wings at Subsonic and Supersonic Speeds. NACA TN 1423, 1947.

2. Ribner, Herbert S., and Malvestuto, Frank S., Jr.: Stability Derivatives of Triangular Wings at Supersonic Speeds. NACA Rep. 908, 1948.

3. Malvestuto, Frank S., Jr., and Margolis, Kenneth: Theoretical Stability Derivatives of Thin Sweptback Wings Tapered to a Point with Sweptback or Sweptforward Trailing Edges for a Limited Range of Supersonic Speeds. NACA TN 1761, 1949.

4. Harmon, Sidney M.: Stability Derivatives at Supersonic Speeds of Thin Rectangular Wings with Diagonals ahead of Tip Mach Lines. NACA Rep. 925, 1949.

5. Jones, Arthur L., and Alksne, Alberta: The Damping Due to Roll of Triangular, Trapezoidal, and Related Plan Forms in Supersonic Flow. NACA TN 1548, 1948.

6. Jones, Arthur L., Spreiter, John R., and Alksne, Alberta: The Rolling Moment Due to Sideslip of Triangular, Trapezoidal, and Related Plan Forms in Supersonic Flow. NACA TN 1700, 1948.

7. Malvestuto, Frank S., Jr., Margolis, Kenneth, and Ribner, Herbert S.: Theoretical Lift and Damping in Roll of Thin Sweptback Wings of Arbitrary Taper and Sweep at Supersonic Speeds. Subsonic Leading Edges and Supersonic Trailing Edges. NACA TN 1860, 1949.

8. Jones, Arthur L., and Alksne, Alberta: The Yawing Moment Due to Sideslip of Triangular, Trapezoidal, and Related Plan Forms in Supersonic Flow. NACA TN 1850, 1949.

9. Cohen, Doris: The Theoretical Lift of Flat Swept-Back Wings at Supersonic Speeds. NACA TN 1555, 1948.

10. Stewart, H. J.: The Lift of a Delta Wing at Supersonic Speeds. Quarterly Appl. Math., vol. IV, no. 3, Oct. 1946, pp. 246-254.

11. Brown, Clinton E.: Theoretical Lift and Drag of Thin Triangular Wings at Supersonic Speeds. NACA Rep. 839, 1946.

12. Brown, Clinton E., and Adams, Mac C.: Damping in Pitch and Roll of Triangular Wings at Supersonic Speeds. NACA TN 1566, 1948.

13. Cohen, Doris: Theoretical Loading at Supersonic Speeds of Flat Swept-Back Wings with Interacting Trailing and Leading Edges. NACA TN 1991, 1949.

14. Walker, Harold J., and Ballantyne, Mary B.: Pressure Distribution and Damping in Steady Roll at Supersonic Mach Numbers of Flat Swept-Back Wings with Subsonic Edges. NACA TN 2047, 1950.

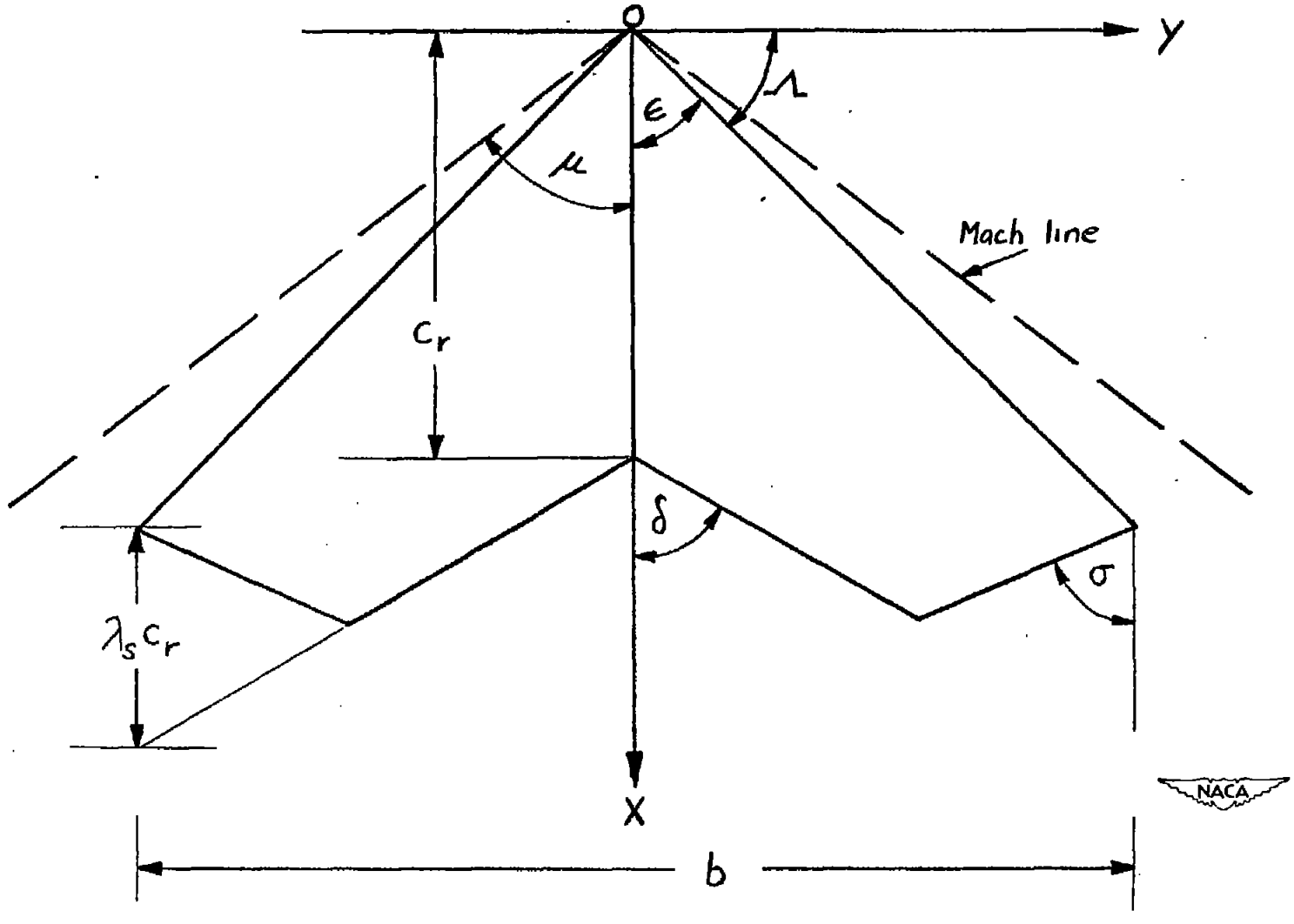

Figure 1.- Sweptback wing with raked-in tip.

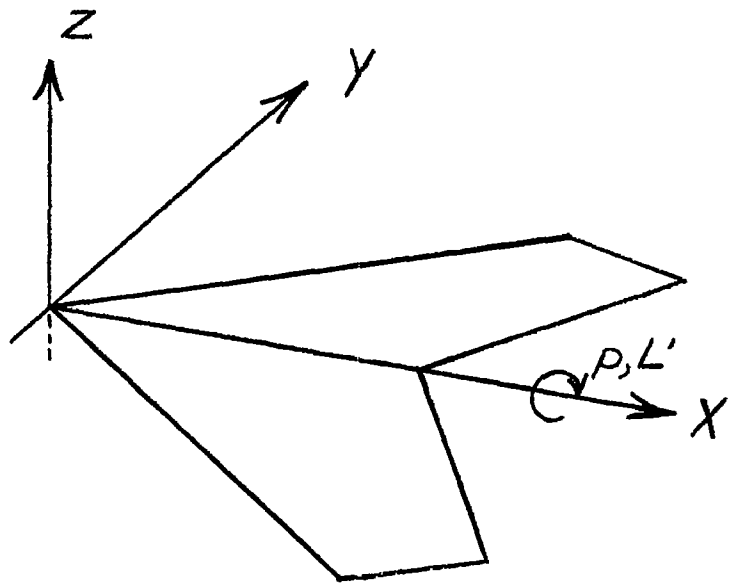

(a) Notation and body axes used in analysis.

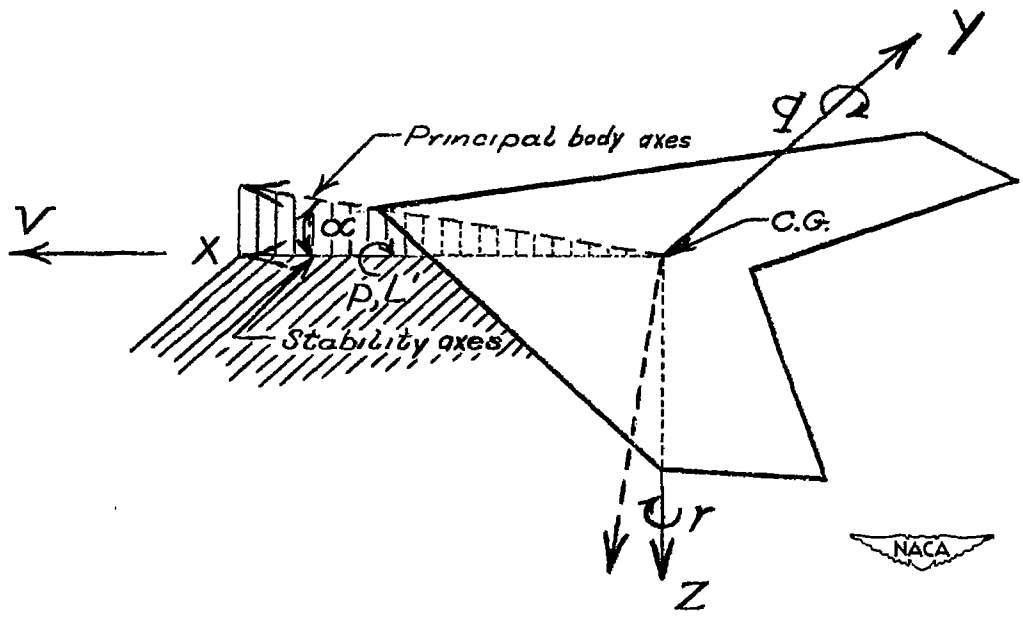

(b) Stability axes. Force and moment arrangement in principal body axes system is identical with that of stability axes system. (Principal body axes dashed in for comparison.)

Figure 2.- System of axes and associated data.

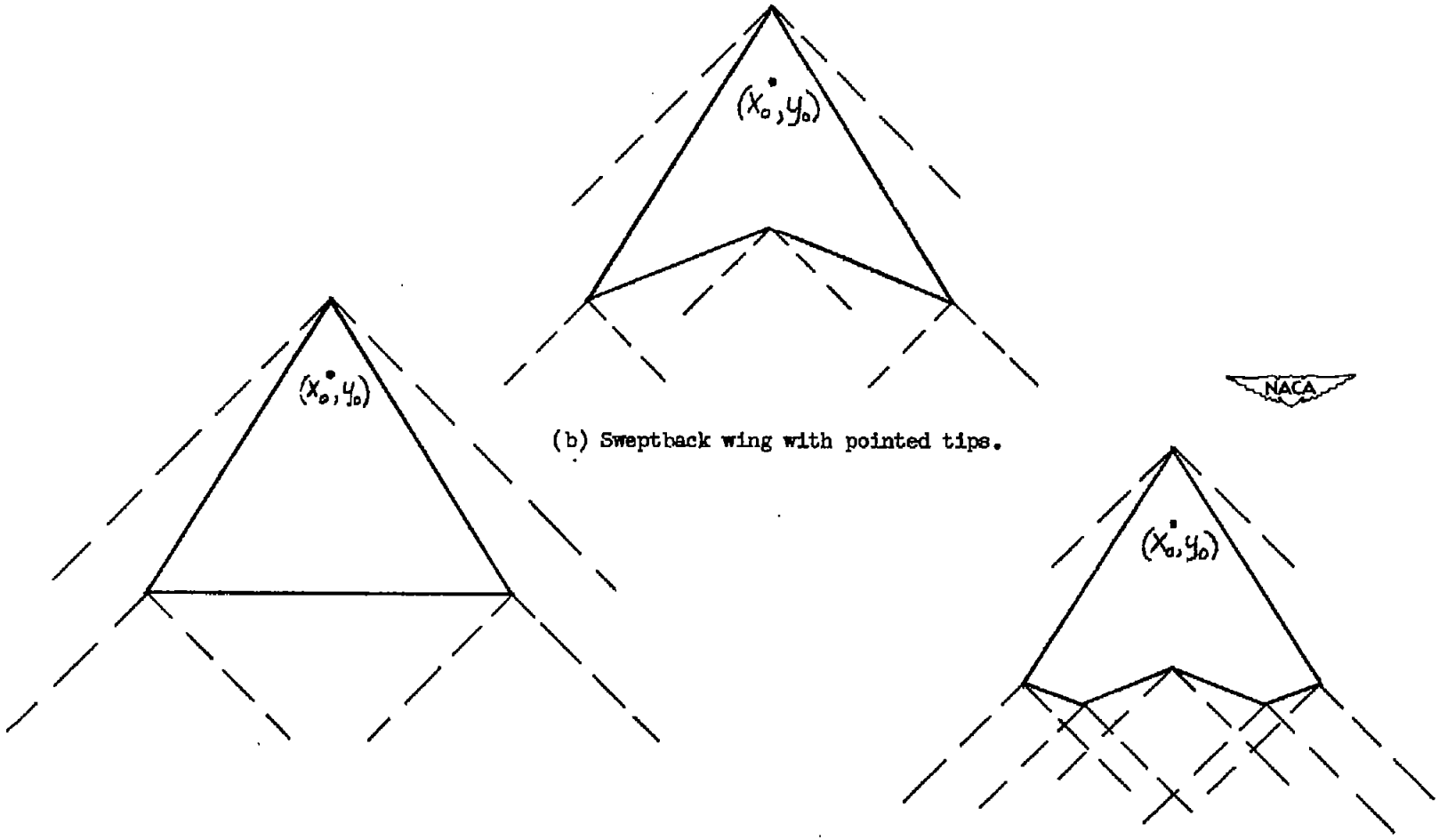

(a) Triangular wing.

(b) Sweptback wing with pointed tips.

(c) Sweptback wing with raked-in tips.

Figure 3.- Wings with identical pressures at corresponding points (for example, at point (x_o, y_o)).

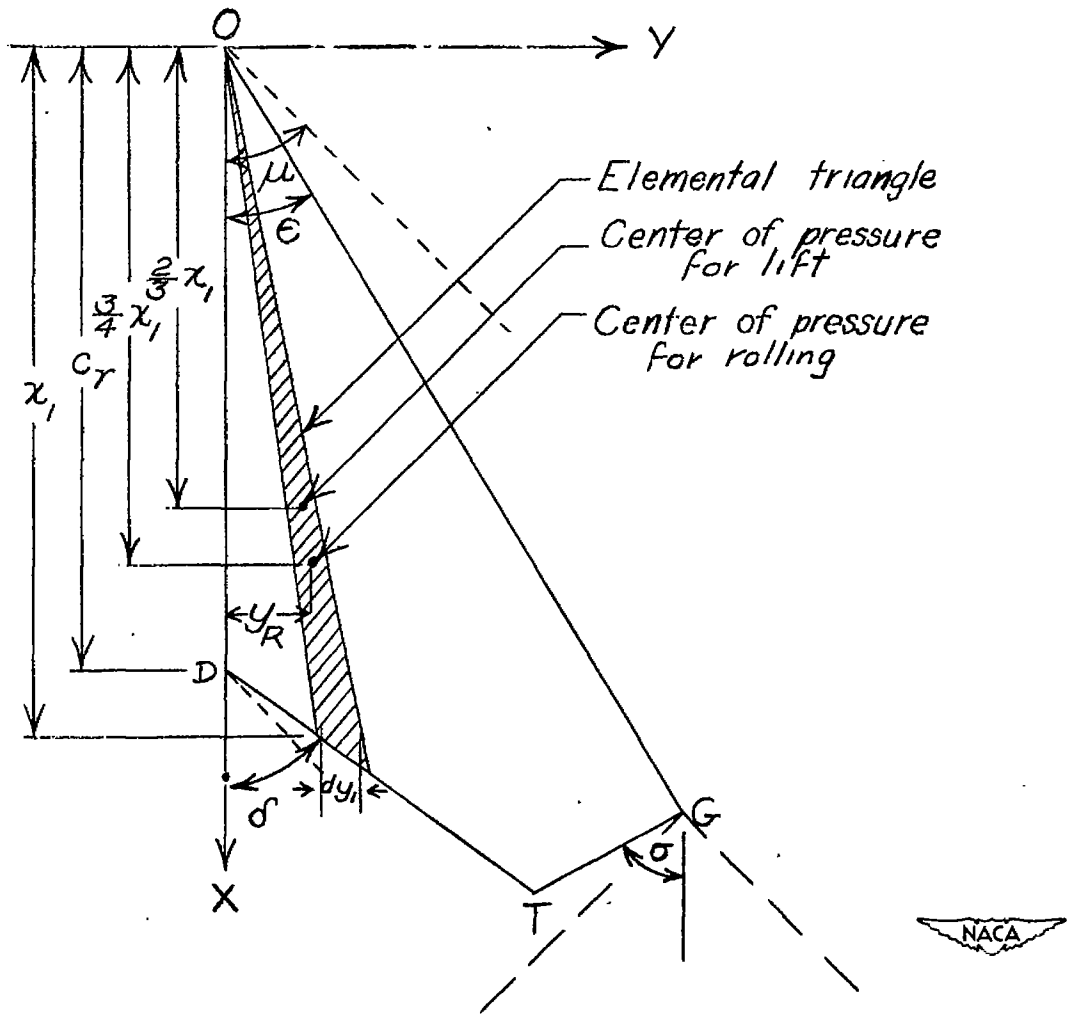

Figure 4.- Sketch of right panel of wing showing an elemental triangle and associated data pertinent to integration limits. Relation for x, y, η: $\eta = \frac{y}{x \tan \epsilon}$ and equation of line connecting O and T:

$$\eta = \frac{m_2}{m_1}\left(\frac{m_1 + m_3 - m_3\omega}{\omega m_2 + m_1 + m_3}\right).$$

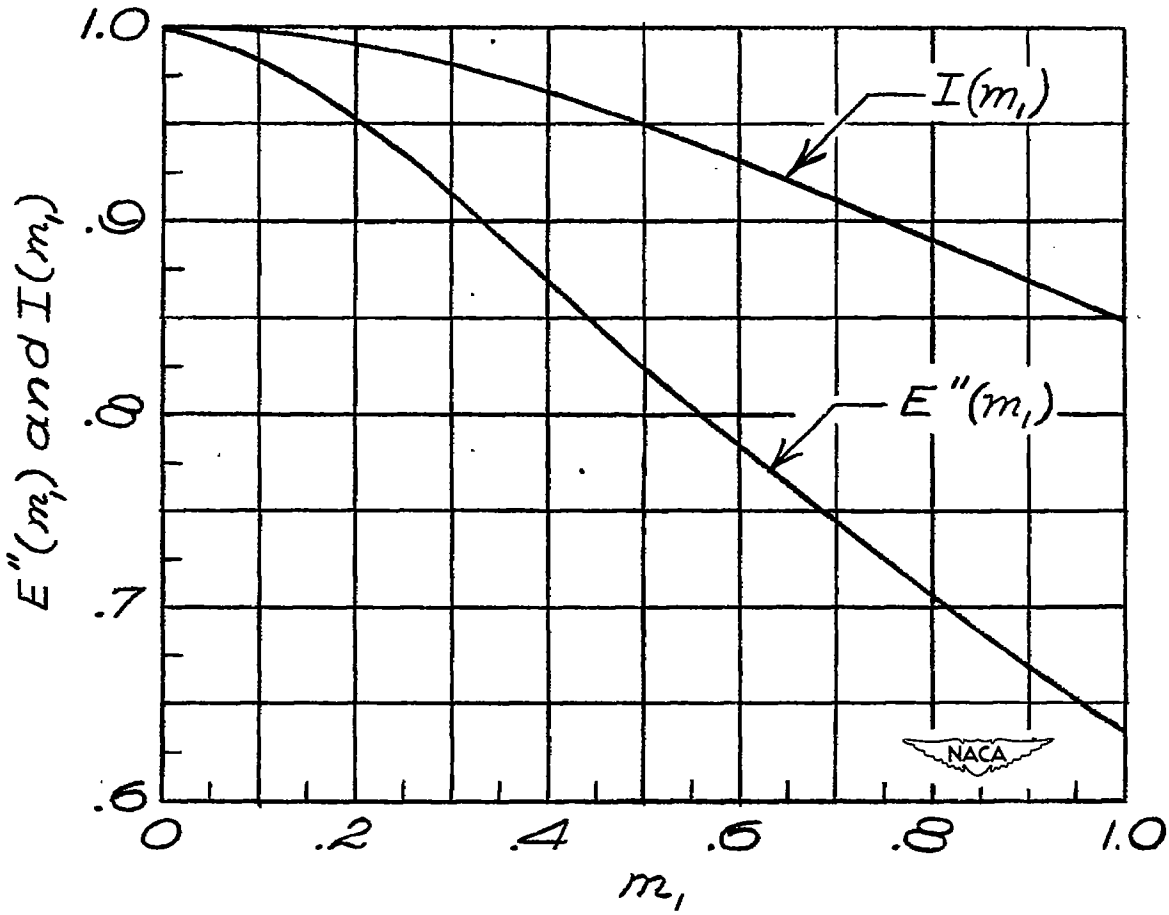

Figure 5.- Variation of the elliptic-integral factors $E''(m_1)$ and $I(m_1)$ with m_1.

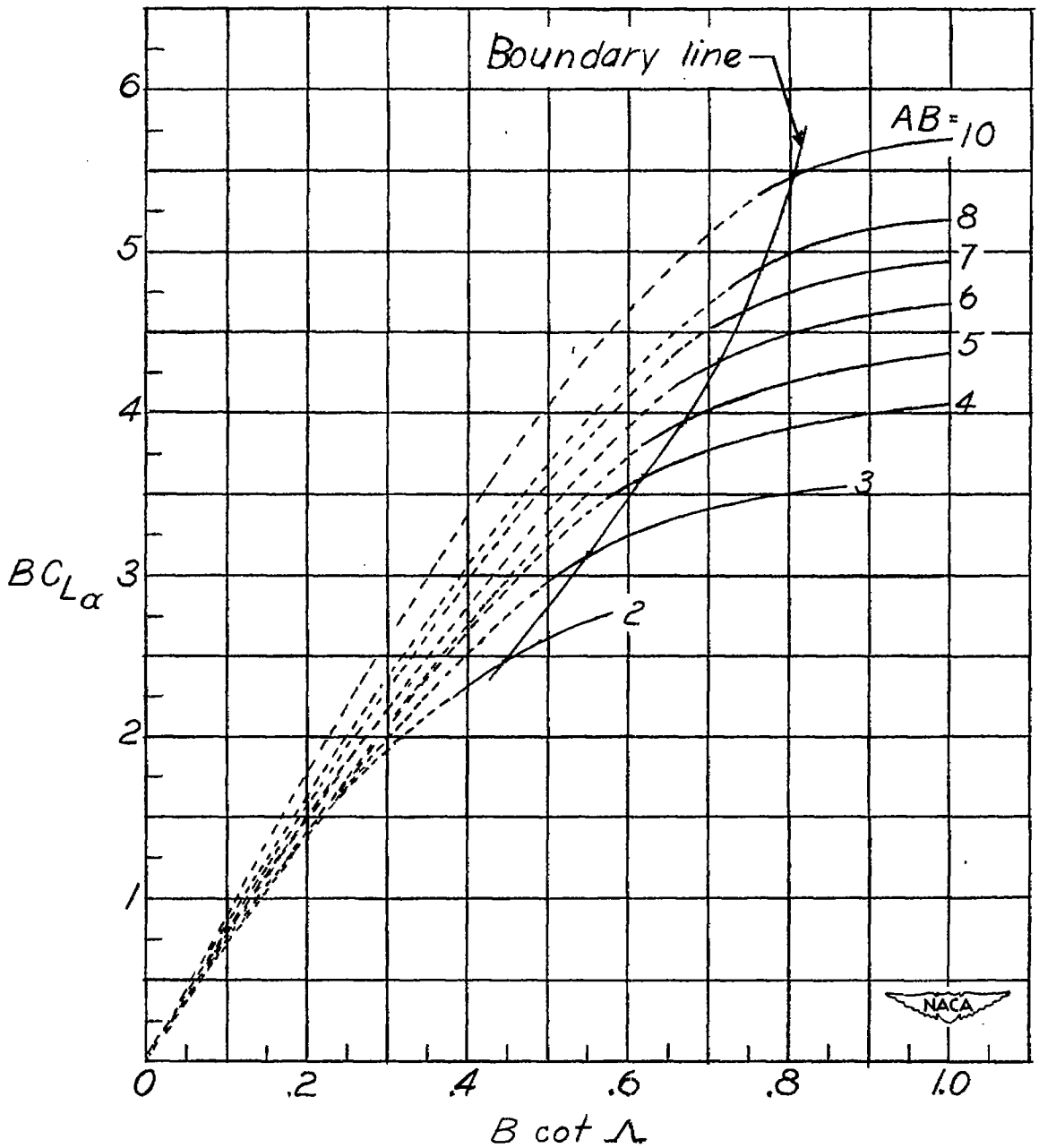

(a) $\lambda_s = 0.25$.

Figure 6.- Variation of BC_{L_α} with B cot Λ for wings with raked-in tips ($\sigma = \delta$). See section entitled "Results and Discussion" for significance of boundary line and dashed portions of curves.

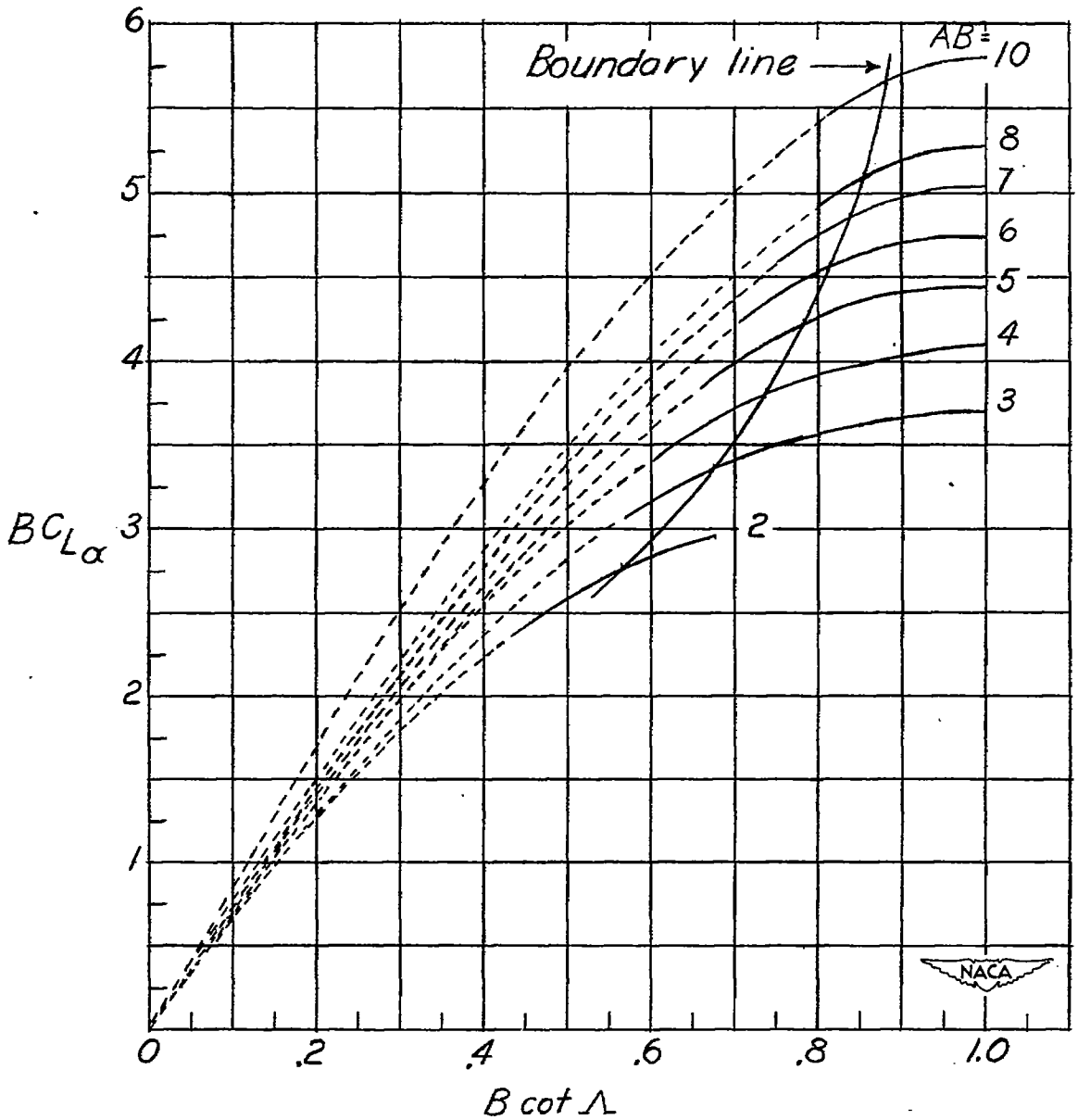

(b) $\lambda_s = 0.50$.

Figure 6.- Continued.

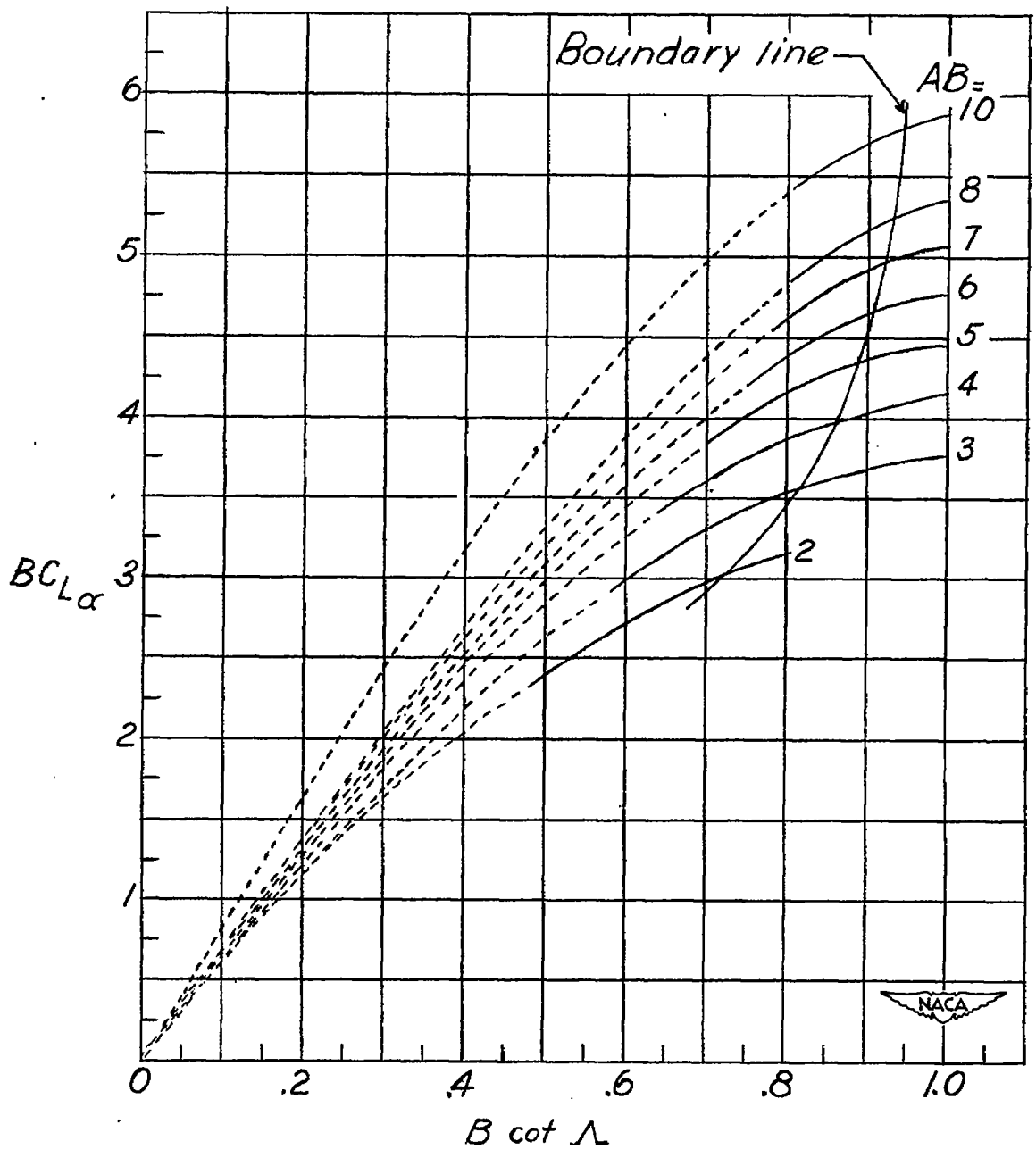

(c) $\lambda_s = 0.75$.

Figure 6.- Concluded.

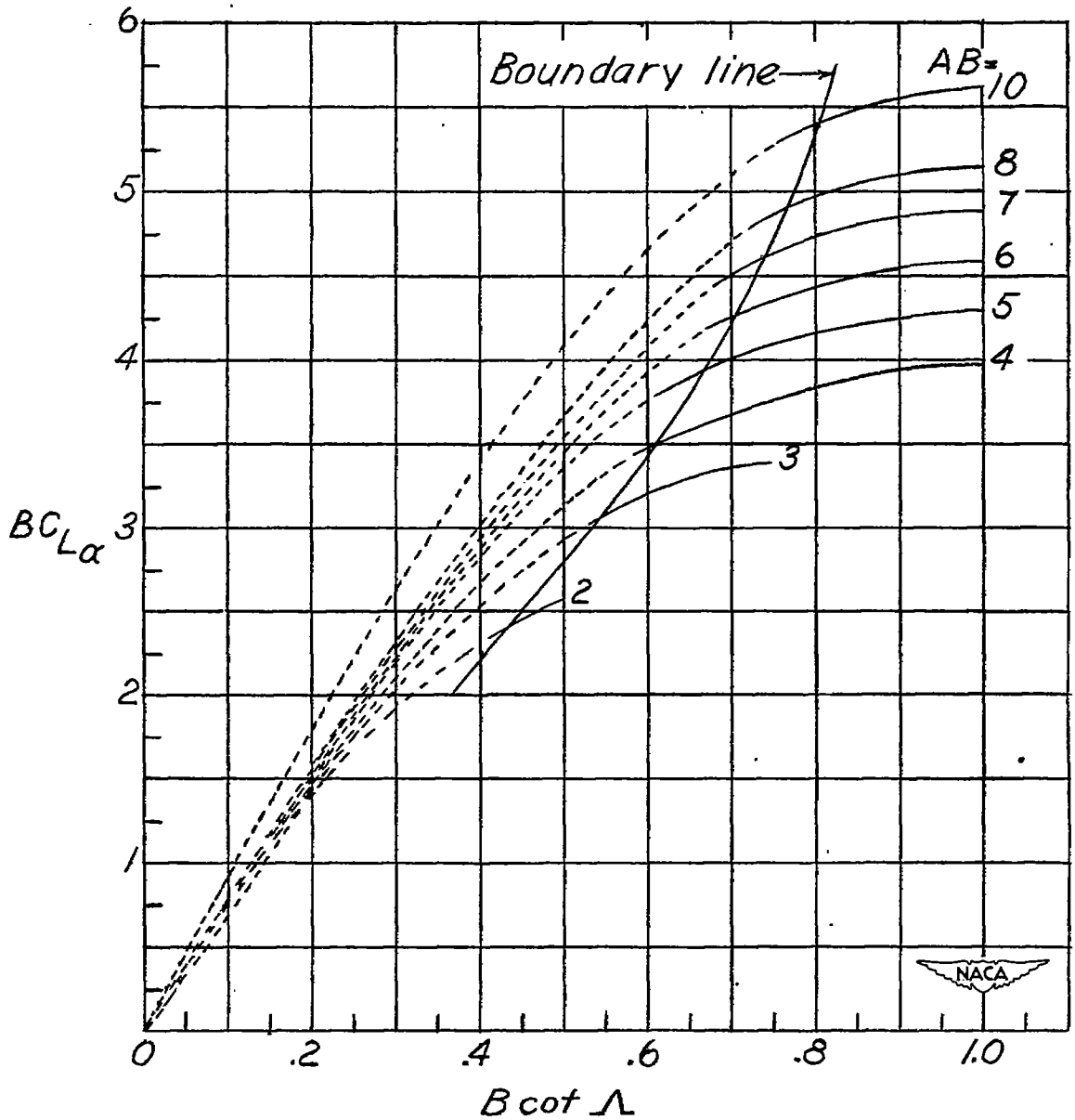

(a) $\lambda_s = 0.25$.

Figure 7.- Variation of BC_{L_α} with B cot Λ for wings with cross-stream tips $\left(\sigma = \frac{\pi}{2}\right)$. See section entitled "Results and Discussion" for significance of boundary line and dashed portions of curves.

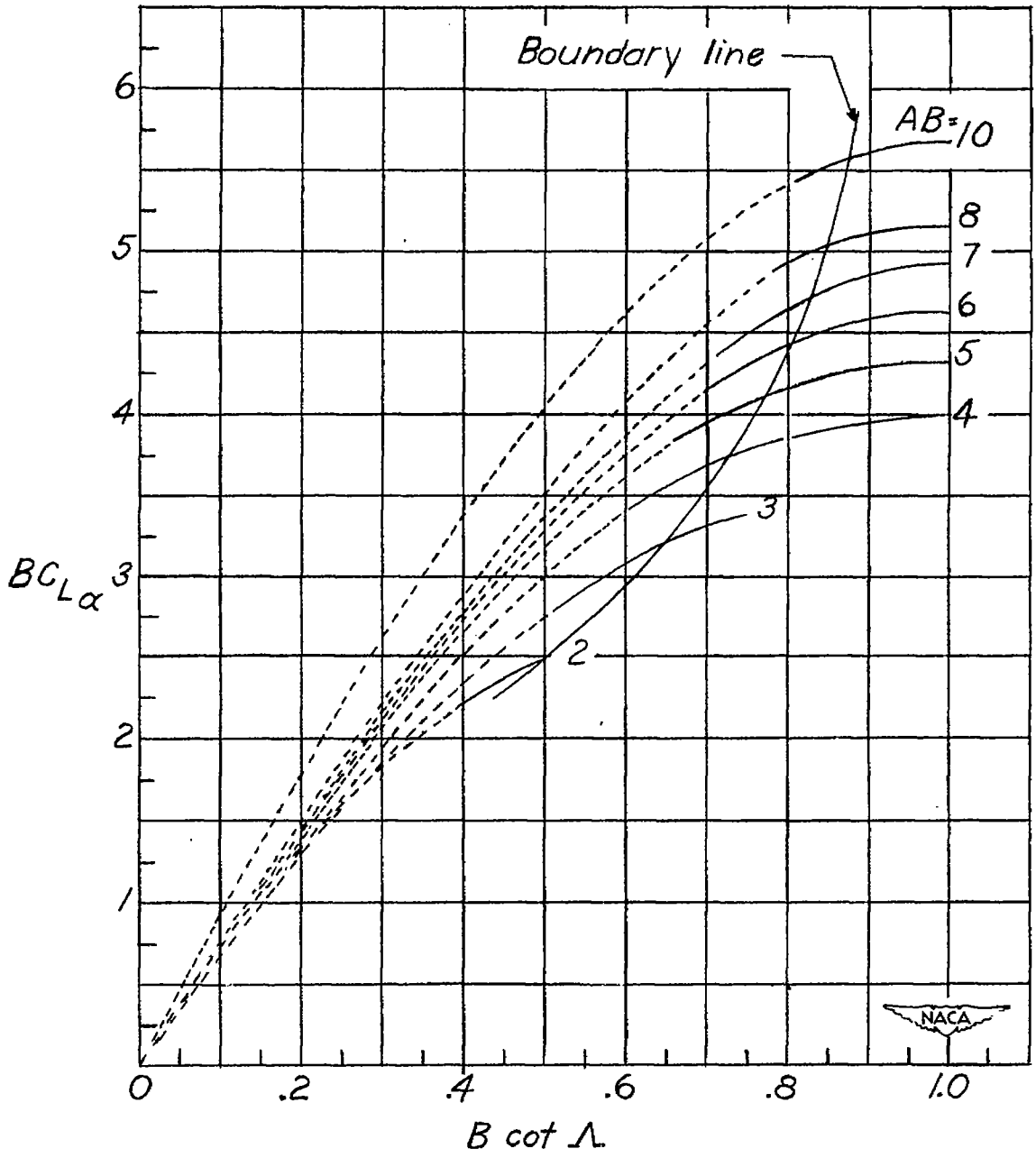

(b) $\lambda_s = 0.50$.

Figure 7.- Continued.

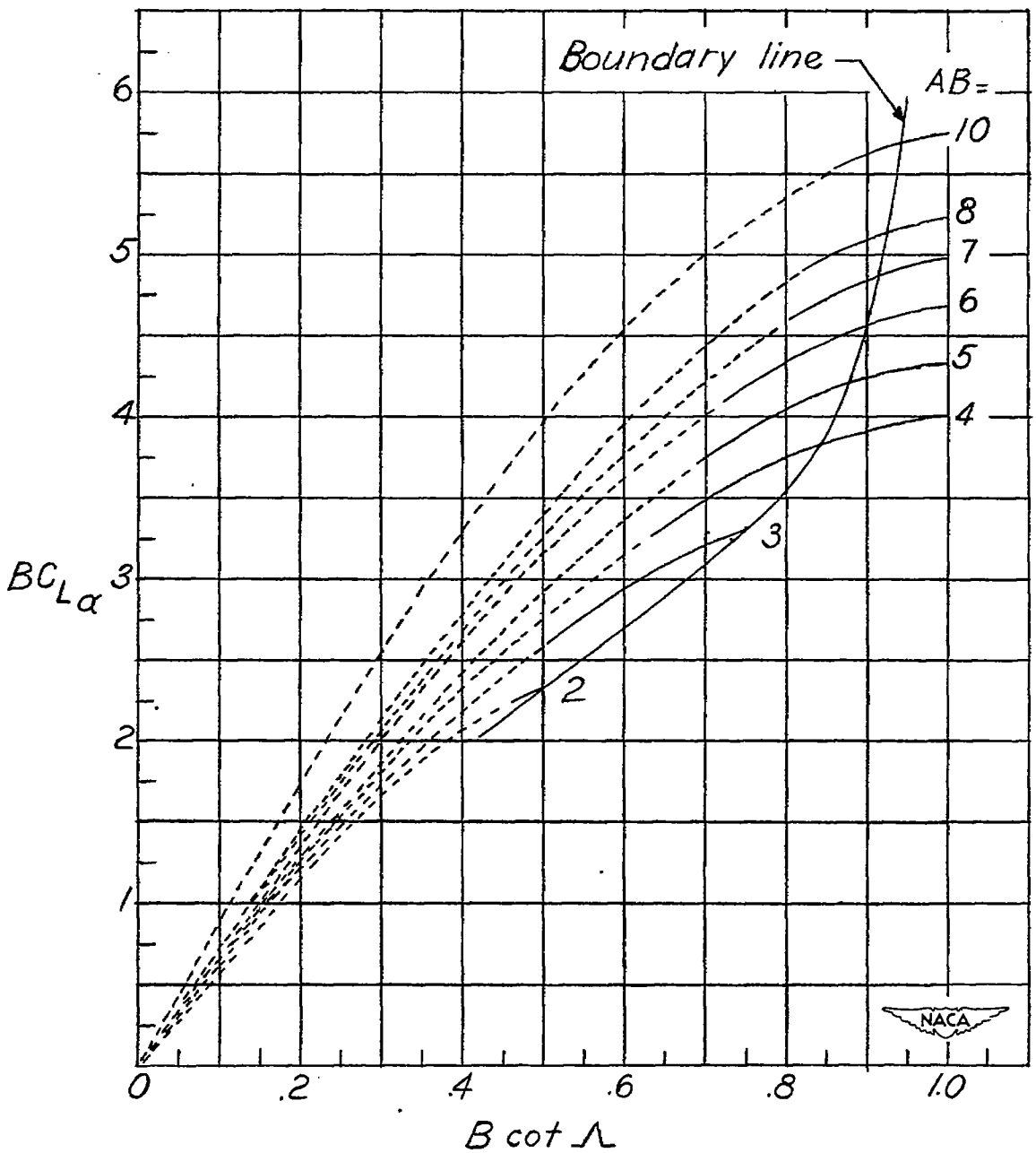

(c) $\lambda_s = 0.75$.

Figure 7.- Concluded.

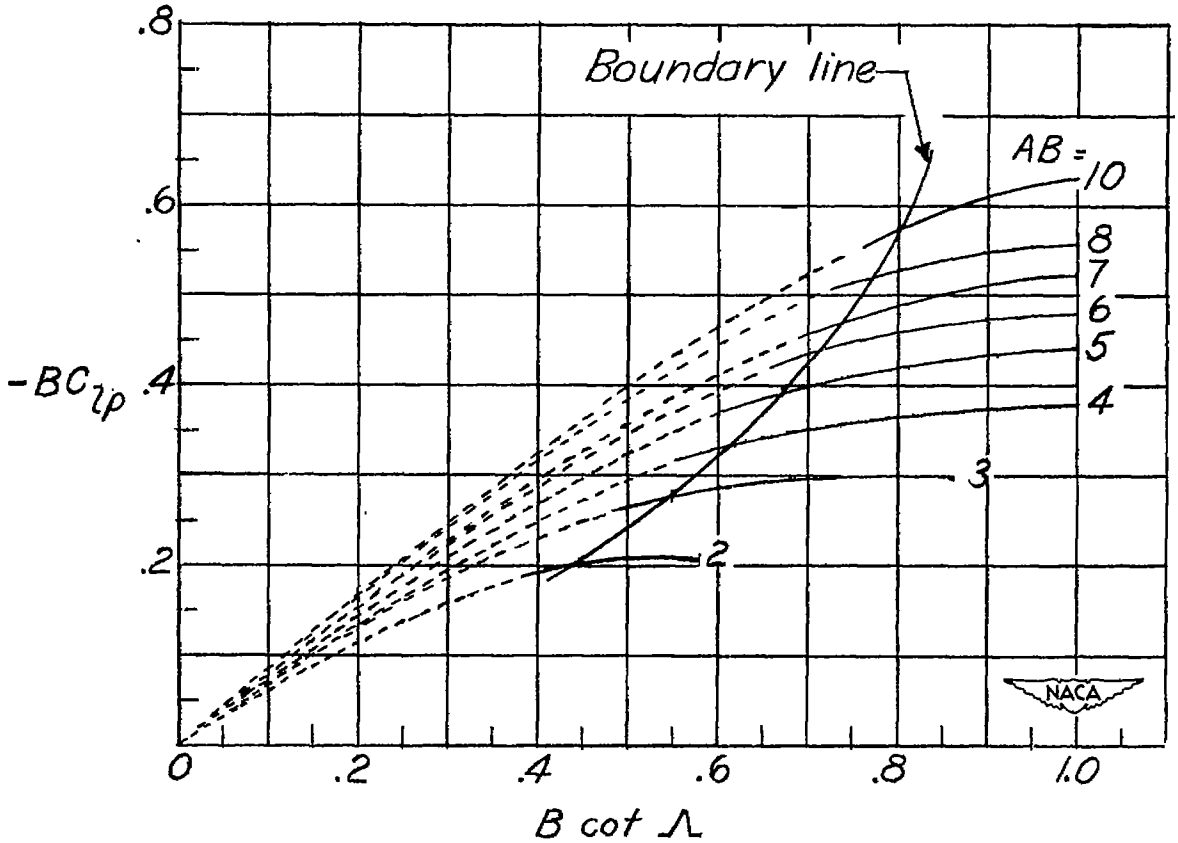

(a) $\lambda_s = 0.25$.

Figure 8.- Variation of $-BC_{l_p}$ with B cot Λ for wings with raked-in tips ($\sigma = \delta$). See section entitled "Results and Discussion" for significance of boundary line and dashed portions of curves.

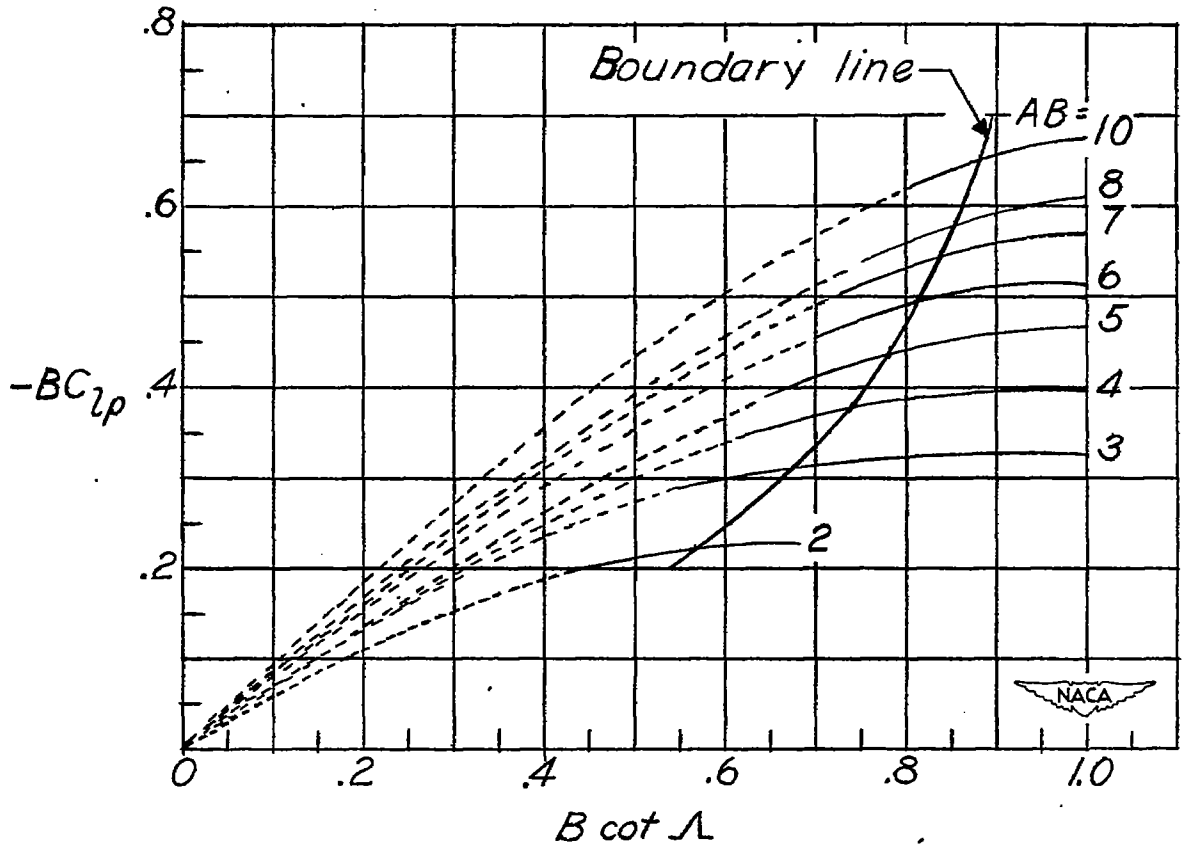

(b) $\lambda_s = 0.50$.

Figure 8.- Continued.

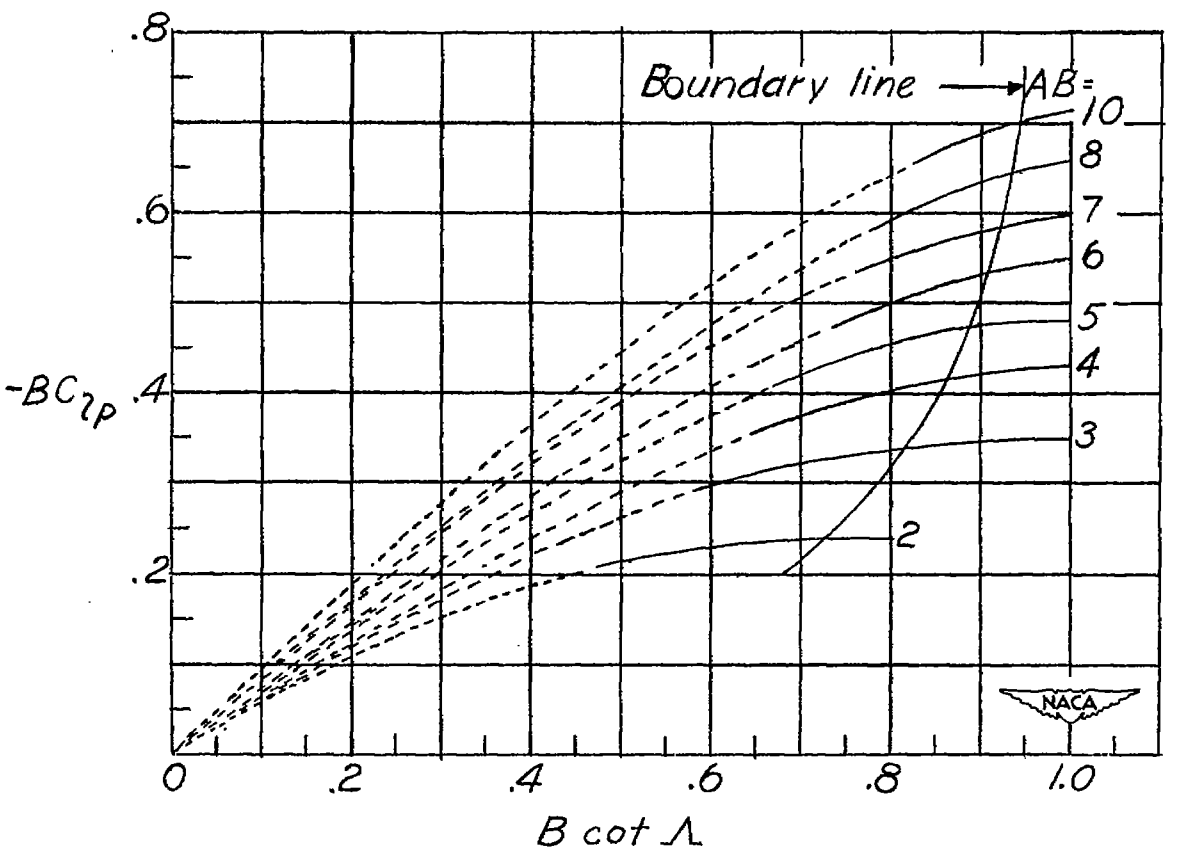

(c) $\lambda_s = 0.75$.

Figure 8.- Concluded.

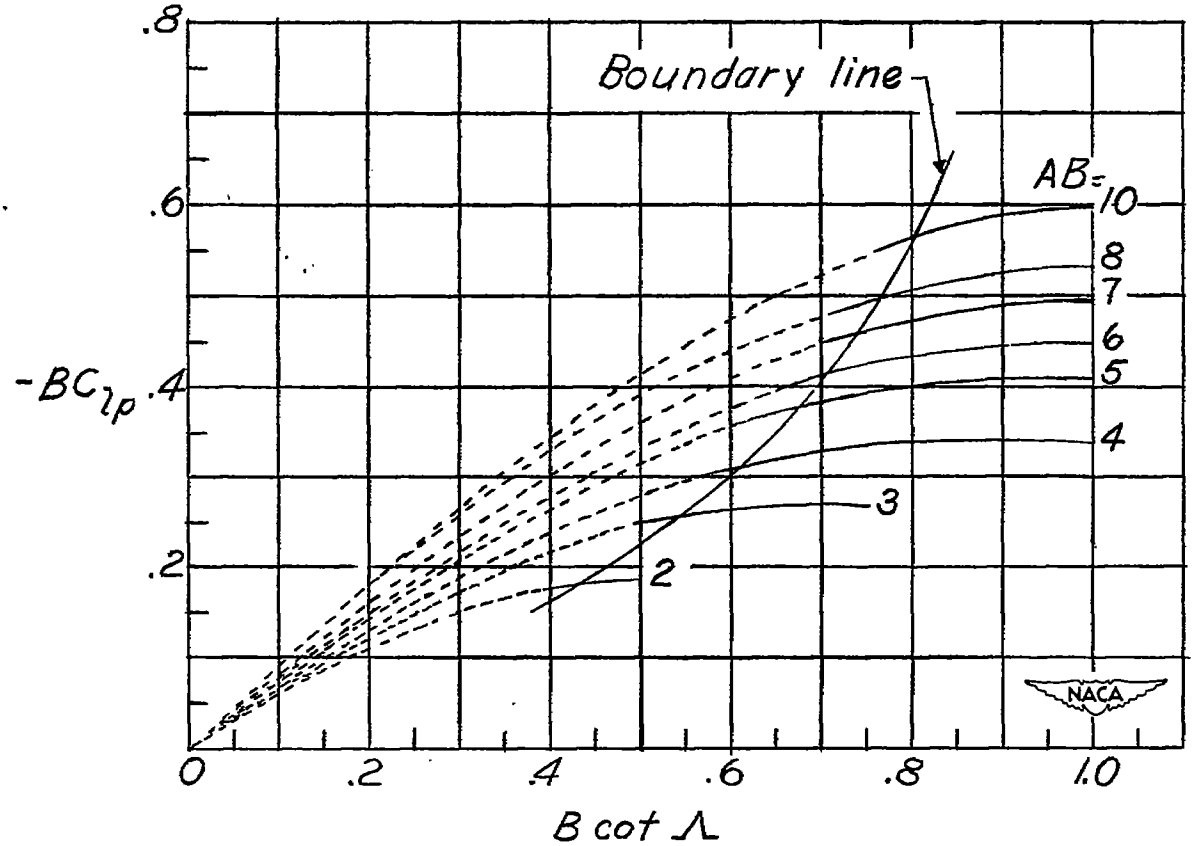

(a) $\lambda_s = 0.25$.

Figure 9.- Variation of $-BC_{l_p}$ with B cot Λ for wings with cross-stream tips $\left(\sigma = \frac{\pi}{2}\right)$. See section entitled "Results and Discussion" for significance of boundary line and dashed portions of curves.

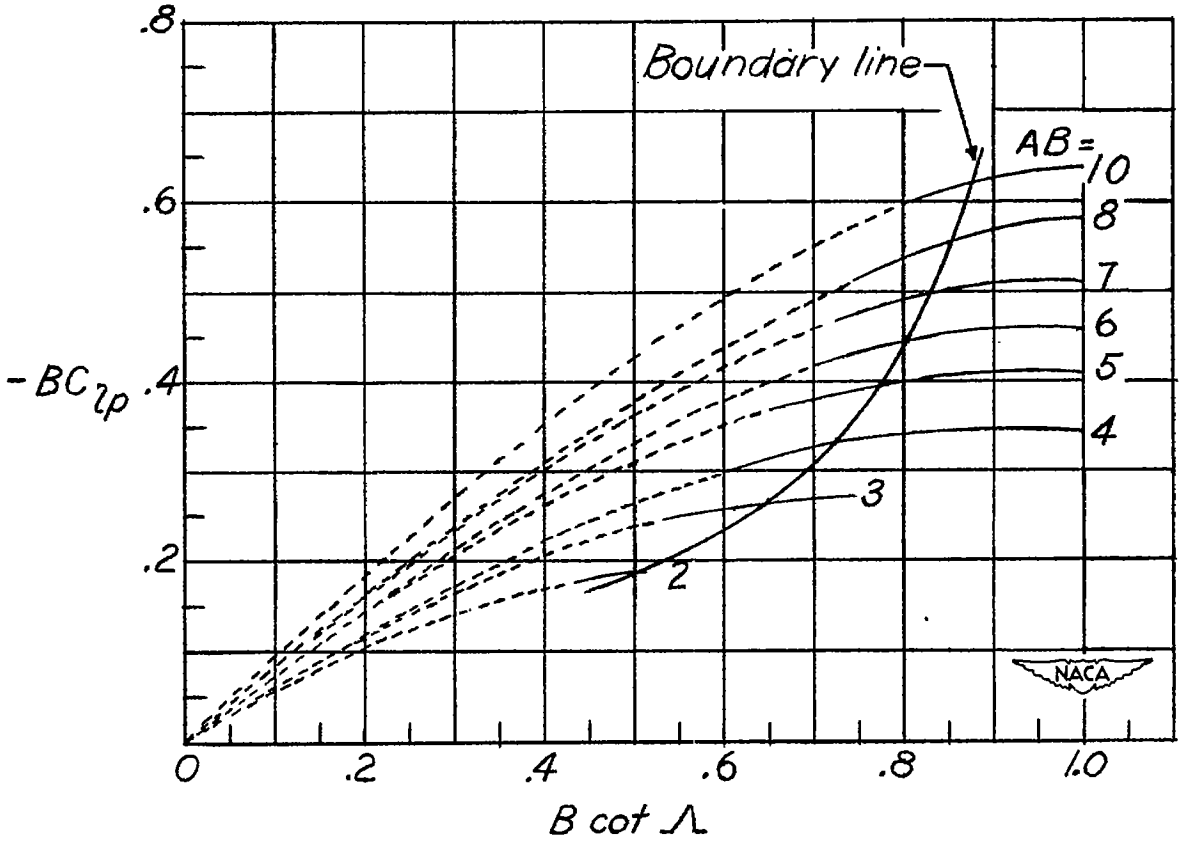

(b) $\lambda_s = 0.50$.

Figure 9.- Continued.

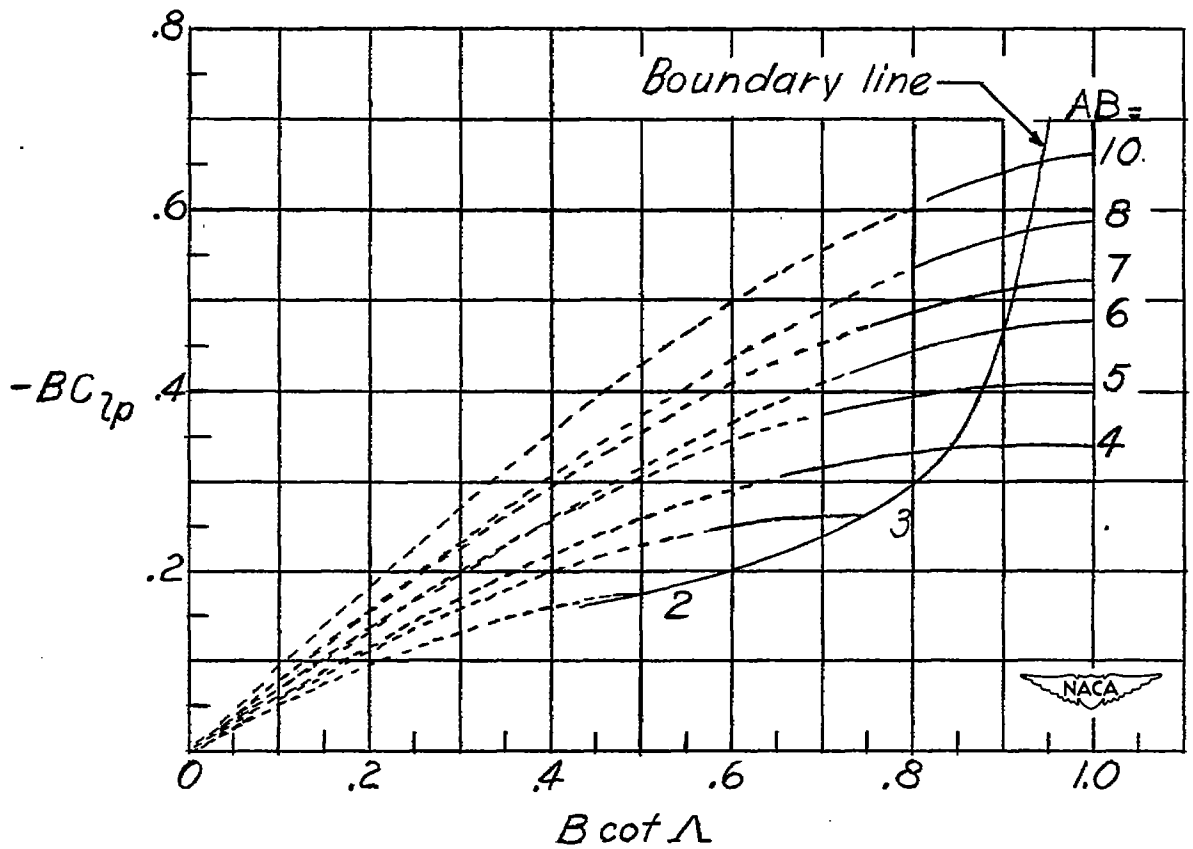

(c) $\lambda_s = 0.75$.

Figure 9.- Concluded.

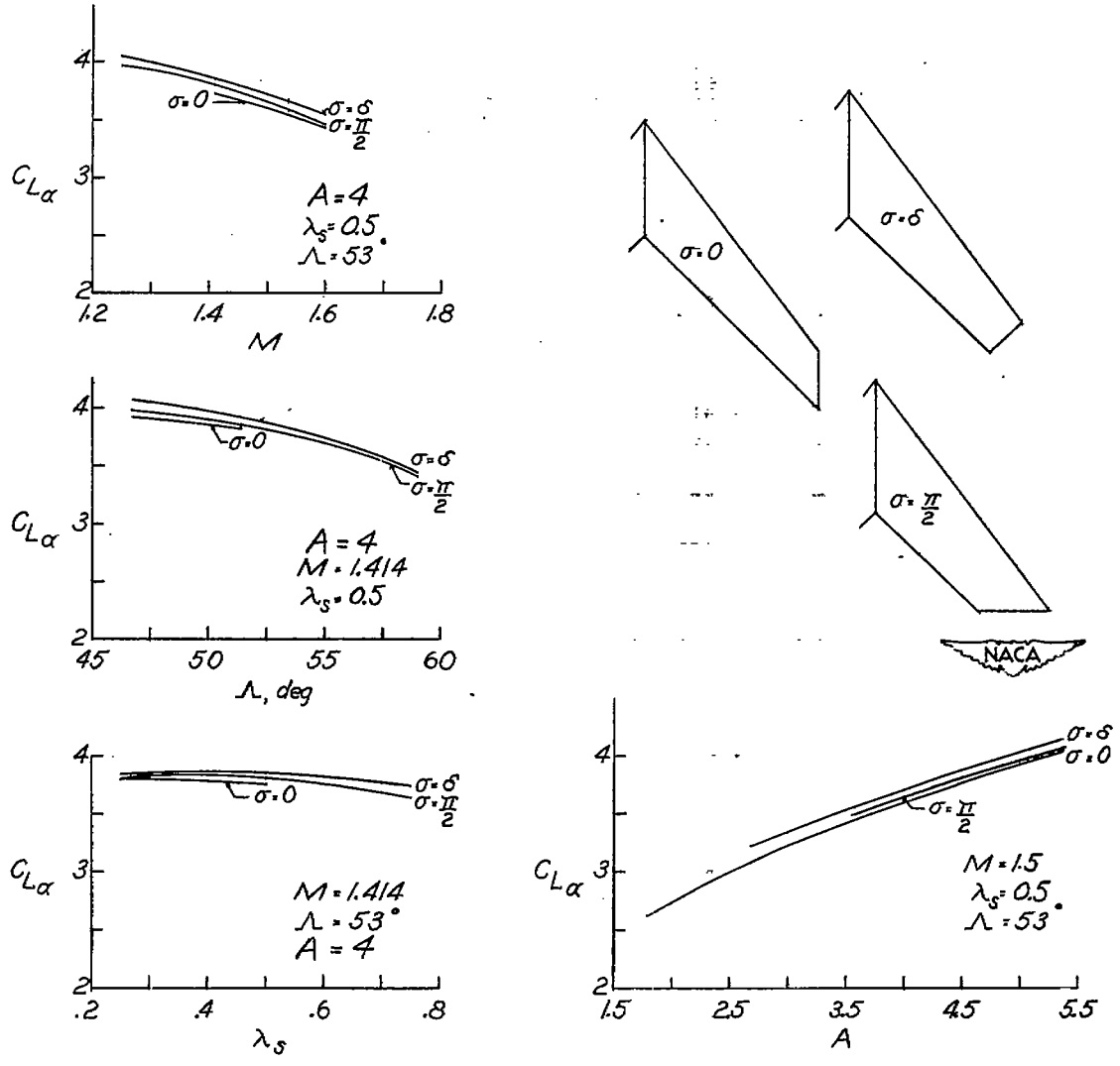

Figure 10.- Some illustrative variations of lift-curve slope C_{L_α} with Mach number, sweepback, taper ratio, and aspect ratio for wings with cross-stream tips $\left(\sigma = \frac{\pi}{2}\right)$, raked-in tips ($\sigma = \delta$), and streamwise tips ($\sigma = 0$ - data from reference 7). Sample wings sketched in figure have following characteristics: $A = 4$, $\lambda_s = 0.5$, $\Lambda = 53°$, and constant wing area.

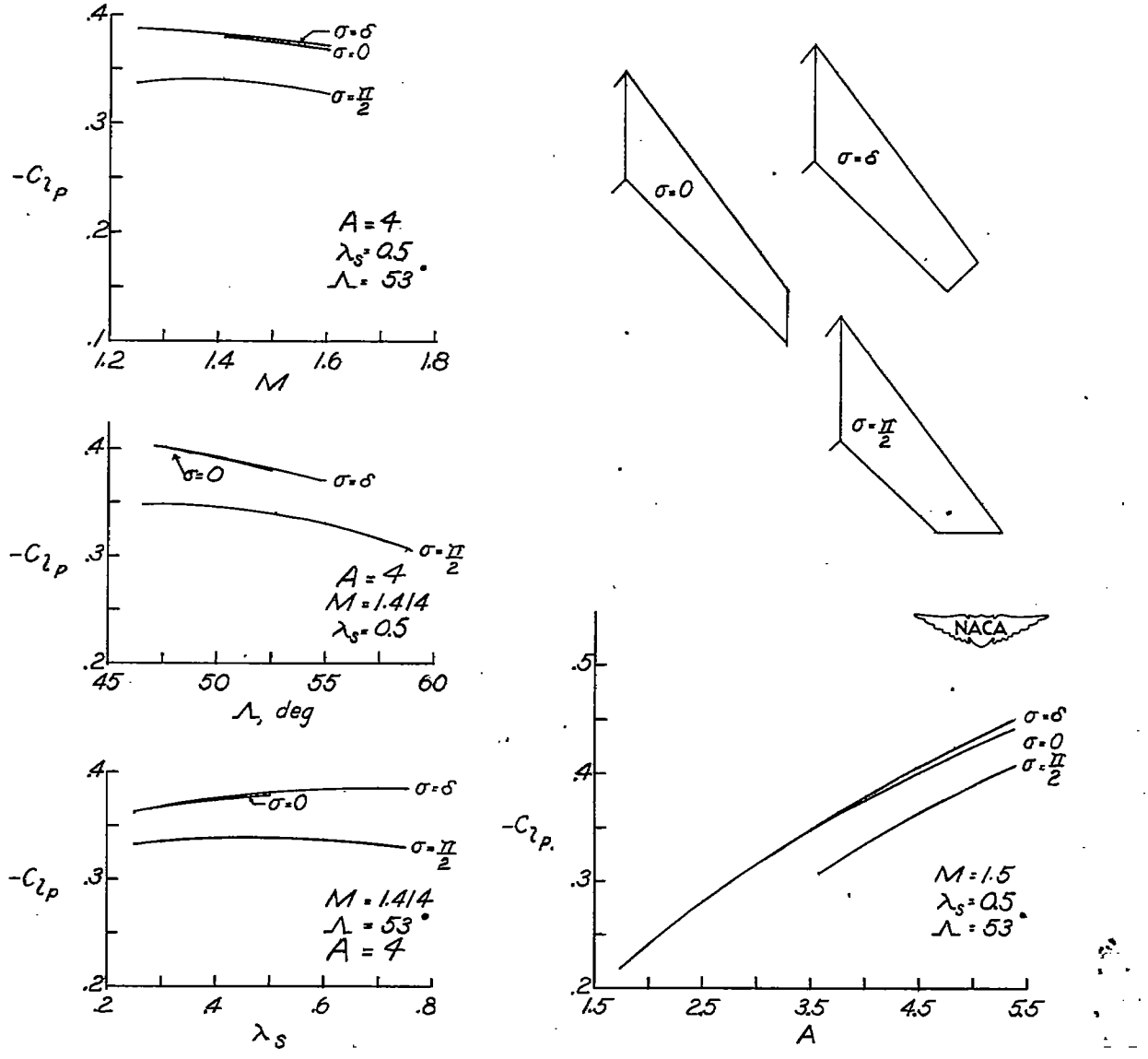

Figure 11.- Some illustrative variations of damping-in-roll derivative $-C_{l_p}$ with Mach number, sweepback, taper ratio, and aspect ratio for wings with cross-stream tips $\left(\sigma = \frac{\pi}{2}\right)$, raked-in tips ($\sigma = \delta$), and streamwise tips ($\sigma = 0$ - data from reference 7). Sample wings sketched in figure have following characteristics: A = 4, λ_s = 0.5, $\Lambda = 53°$, and constant wing area.